The Astrophysical Journal, 843:56 (6pp), 2017 July 1 https://doi.org/10.3847/1538-4357/aa77f9

The 9577 and 9632 Å Diffuse Interstellar Bands: C_{60}^+ as Carrier

G. A. H. Walker[1], E. K. Campbell[2], J. P. Maier[2], and D. Bohlender[3]
[1] 1234 Hewlett Place, Victoria, BC V8S 4P7, Canada; gordonwa@uvic.ca
[2] Department of Chemistry, University of Basel, CH-4056 Basel, Switzerland; ewen.campbell@unibas.ch, j.p.maier@unibas.ch
[3] National Research Council of Canada, Herzberg Astronomy and Astrophysics, 5071 West Saanich Road, Victoria, BC V9E 2E7, Canada; david.bohlender@nrc-cnrc.gc.ca
Received 2017 April 25; revised 2017 June 2; accepted 2017 June 5; published 2017 July 3

Abstract

Galazutdinov et al. (2017) recently claimed that the relative strengths of the 9577 and 9632 Å diffuse interstellar bands (DIBs) are too poorly correlated to be caused by a single source, the C_{60}^+ ion. Their conclusion is based on theoretical modeling of contaminating stellar Mg II lines at 9631.9 and 9632.4 Å and UVES spectra. This contradicts their earlier result and those of several others that the two DIBs are closely correlated and, within the errors and effects of stellar blends, exhibit an intensity ratio consistent with that found in the 6 K laboratory spectrum of C_{60}^+. We consider the use of close spectral standards to be superior to model atmosphere calculations in correcting for contamination by the Mg II lines. We have examined some of the same UVES spectra and demonstrate that a lack of suitably observed telluric standards makes it impossible to adequately correct for telluric water vapor contamination, leading to unreliable continuum levels. The possible effects of higher temperatures, in the 30–100 K range, on the C_{60}^+ electronic absorption band profiles, and their relative intensities, are also considered.

Key words: ISM: molecules

1. Introduction

On the basis of the absorption spectrum of C_{60}^+ measured in a 5 K neon matrix (Fulara et al. 1993), Foing & Ehrenfreund (1994) searched for diffuse interstellar bands (DIBs) in the wavelength region predicted for the gas phase. They found two new DIBs within this range and made the suggestion that the fullerene ion C_{60}^+ is responsible for these absorptions at 9577 and 9632 Å. Twenty years later, laboratory spectroscopy confirmed the proposition (Campbell et al. 2015) based on photofragmentation spectra of C_{60}^+–He complexes at 6 K. Since then, Campbell et al. (2016b) determined the perturbation caused to the C_{60}^+ wavelengths due to the weakly bound helium atom, and Walker et al. (2016) demonstrated that using these wavelengths improves the coincidence with the 9632, 9577, 9428, 9365, and 9348 DIBs.

The wavelengths listed in Table 1 of Campbell et al. (2015), as stated there, are for C_{60}^+–He. In that study, the measurement of one of the strong absorption bands for C_{60}^+–He_2 under the same conditions was reported. For the band at 9577 Å the wavelengths of C_{60}^+–He and C_{60}^+–He_2 were found to agree within 0.2 Å, providing an indication that the values for C_{60}^+–He are close to those of C_{60}^+ itself. Subsequently, improvements to the experimental apparatus allowed lower trap temperatures to be achieved, enabling the formation of C_{60}^+ complexes with several helium atoms attached. It was then discovered that the central wavelengths of the C_{60}^+–He_n spectra depend slightly on the experimental conditions (see Campbell et al. 2016b for a discussion). However, the data recorded for $n = 1-3$ at the lowest cryogenic temperature revealed an approximately linear behavior of the central wavelengths with n (their Figure 2). Their extrapolation provides a more accurate estimate of the wavelengths of bare C_{60}^+. These were reported with a ±0.2 Å uncertainty as determined from a linear fit to the $n = 1-3$ data. In independent laboratory experiments, Kuhn et al. (2016) measured the photofragmentation spectra of C_{60}^+–He_n ($n = 2-32$) in helium nanodroplets. The wavelengths predicted for the absorption of C_{60}^+ were found to be in accord with the values stated in Campbell et al. (2016b). It should be pointed out that the 0.37 K internal temperature of ions in the helium droplet experiment is lower than in the ion trap (6 K). The influence of temperature on the C_{60}^+ absorption band characteristics is further discussed in Section 2.

Subsequent to the Foing & Ehrenfreund (1994) paper, there were several observational studies of the 9577 and 9632 DIBs and their relative intensities (Foing & Ehrenfreund 1997; Jenniskens et al. 1997; Galazutdinov et al. 2000, 2017; Herbig 2000; Misawa et al. 2009; Cox et al. 2014). The results up to 2016 are summarized in Campbell et al. (2016b). The most extensive of these studies in terms of the number of lines of sight investigated, by Galazutdinov et al. (2000, p. 752), sets out the complications introduced by the presence of strong telluric water vapor (WV) lines in establishing intrinsic DIB profiles. To quote from their paper, "The difficult problem is the strong telluric contamination of the investigated spectral range. The telluric lines are in many cases almost saturated, which makes it impossible to remove them by division with the telluric standard. Any attempt to do this by means of re-scaling the depths of these features can affect the continuum level, especially close to "empty" regions, i.e., the close vicinities of both the 9632 and 9577 Å features." In addition, Jenniskens et al. (1997) pointed out that in late B stars, the 9632 DIB coincides with a pair of Mg II stellar lines at 9631.9 and 9632.4 Å so the profiles must be corrected for this blend before comparison with the laboratory profiles.

To correct for both the telluric and the stellar line contamination one must observe, as a telluric standard, a star whose lines are greatly broadened by stellar rotation closely in time and air mass to those of the target star. In addition, observations are required of an unreddened star of a similar spectral type as the target to compensate for the stellar Mg II lines. In the reduction, both the spectral standard and the target

spectra are divided by the telluric reference with some scaling, if necessary, before shifting the former to match the radial velocity of the target. Finally, the corrected target spectrum is shifted in wavelength by the reflex of the interstellar velocity—generally determined from the interstellar K line at 7699.0 Å.

While all of the observations of the 9632 and 9577 DIBs except those of Cox et al. (2014) followed the above steps, Galazutdinov et al. (2017) introduced corrections for the Mg II line contamination based on line profiles from model atmosphere calculations.

2. The 9632/9577 DIB Equivalent Width Ratio

2.1. Laboratory Prediction

Based on laboratory measurements of C_{60}^+–He, the C_{60}^+ absorption bands at 9632 and 9577 were reported to originate from the lowest vibrational level of the ground electronic state, which is assigned as $^2A_{1u}$ in an assumed D_{5d} symmetry (Campbell et al. 2015). This implies that these are transitions to two upper states separated in energy by around 60 cm^{-1}. Due to the experimental method used, the laboratory measurements could only be recorded at a 6 K internal (rotational) temperature. Our interpretation is that the ∼2.5 Å FWHM of the bands at this temperature is caused by a ∼2 ps lifetime of the excited state(s) because the expected FWHM of the rotational envelope at 6 K is only 1 Å by comparison with the simulations carried out for C_{60} (Edwards & Leach 1993). Here we consider the influence of temperature on the wavelengths and band profiles of the 9577 and 9632 absorptions because values above 6 K, in the range 30–100 K (as determined by the gas kinetic temperature), are more relevant for nonpolar C_{60}^+ in the diffuse clouds. For example, C_3 (Maier et al. 2001) and H_3^+ (Indriolo et al. 2007) have temperatures in the range of 30–80 K. Of interest for comparison with astronomical observations is whether differences between the rotational constants in the two excited electronic states could result in changes to the characteristics of the absorption bands.

Simulations of the rotational envelopes of neutral and charged fullerene transitions have been reported several times (Weeks & Harter 1991; Edwards & Leach 1993; Sogoshi et al. 2000). Recently, Yamada et al. (2017) calculated the rotational constants of $^{12}C_{60}^+$ in D_{5d} symmetry using density functional theory. For this symmetric top molecule they give $A = 84.22$ MHz and $B = 83.26$ MHz. We have carried out simulations of the rotational profile of a $^2E_{1g} \leftarrow {}^2A_{1u}$ electronic transition in D_{5d} symmetry with these constants for both the lower and the upper states using PGOPHER (Western 2016). With a 1% decrease in the excited state rotational constants there is a shift of ∼0.6 Å to the wavelength of the band maximum (of profiles that are lifetime broadened) when increasing the temperature from 6 to 100 K. This shift increases to ∼1.1 Å for a 2% reduction in A' and B'. The change in the A and the B constants upon ionization, C_{60} $(I_h) \rightarrow C_{60}^+(D_{5d})$, is 1.5% and 0.3%, respectively (Yamada et al. 2017). We do not know what the differences are between the rotational constants in the two upper electronic states (9577 and 9632 bands). Consequently, it is difficult to reach a firm conclusion on the effect this will have at temperatures greater than the 6 K laboratory spectrum. One can get some idea of the possibilities by looking at the simulations made for a variety of changes to the constants in Edwards & Leach (1993) for C_{60}. Small differences in the wavelengths and appearance of the DIB profiles, caused by the C_{60}^+ rotational envelopes, should be considered in the analysis of lines of sight that sample high and low rotational temperature environments. Already in 1997 it was suggested that the rotational temperature for HD 37022 could be a factor of 2 higher than for HD 183143 (Foing & Ehrenfreund 1997).

Table 1
Wavelengths, Absolute Absorption Cross-sections, and Uncertainties Inferred for the Near Infrared C_{60}^+ Bands at 6 K Based on Laboratory Measurements[a]

λ_c/Å	$\sigma/\times 10^{-15}$ cm^2
9632.1 ± 0.2	4 ± 2
9577.0 ± 0.2	5 ± 2
9427.8 ± 0.2	1.4 ± 0.5
9365.2 ± 0.2	1.2 ± 0.4
9348.4 ± 0.2	0.4 ± 0.2

Note.
[a] Wavelengths are taken from Campbell et al. (2016b). Absolute cross-sections for the two strongest bands were measured in a 4-pole ion trap as described in Campbell et al. (2016a). σ values and uncertainties for the three weaker bands are based on relative intensity data obtained from earlier experiments using a 22-pole ion trap (Campbell et al. 2015).

In the laboratory study at 6 K by Campbell et al. (2015), relative absorption cross-sections of 0.8 and 1 were inferred for the C_{60}^+ bands at 9632 and 9577, respectively, and were reported with an estimated uncertainty of about 20%, following experiments made using a 22-pole ion trap. In order to determine absolute cross-sections, a purpose-built cryogenic 4-pole trap was used instead in which the ion cloud could be compressed to ensure good overlap with the laser beam. The details have been reported in Campbell et al. (2016a), where the evaluation of systematic uncertainties in the determination of cross-sections is discussed. These arise due to such factors as the reproducibility of the laser-ion cloud overlap and the measurement of the irradiation time and laser power. We note that Figures 1 and 3 in Campbell et al. (2015, 2016a), respectively, were included to illustrate the wavelengths and approximate strengths of the C_{60}^+ bands at 6 K. For a detailed comparison with the DIB wavelengths and EWs, assuming that the latter have been reliably determined at a similar temperature, we recommend using the values listed in Table 1, along with their associated uncertainties. Note that these values are consistent with the relative intensities reported in previous work (Campbell et al. 2015, 2016a). For completeness, the absolute values of the weaker C_{60}^+ features near 9348, 9365, and 9428 Å are also included.

Recently, spectroscopic measurements of the near-infrared electronic absorptions of C_{60}^+ with different weakly bound ligands attached, including H_2, D_2 and rare gas atoms, were reported (Holz et al. 2017). One observation that may have implications for C_{60}^+ itself is the "splitting" of the absorption bands, particularly noticeable in the region around 9632 Å (their Figure 1). A possible explanation is that there are low-lying excited electronic state(s), populated even at low (<10 K) temperatures, as suggested following magnetic circular dichroism experiments. The energy difference of these from the ground $^2A_{1u}$ state is expected to be only a few cm^{-1} (Langford & Williamson 1999). Due to the Jahn–Teller effect, the symmetry of C_{60}^+ is reduced from I_h (as for C_{60}) to D_{5d}. An electronic state correlation diagram connecting these representations is shown in Figure 1. Upon descent in symmetry, the ^2H_u

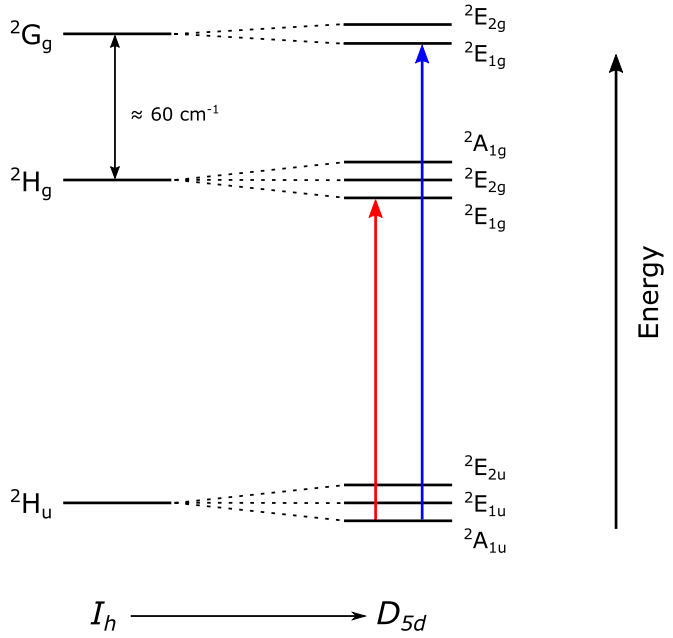

Figure 1. Electronic state correlation diagram for the reduction in symmetry from I_h (left) to D_{5d} (right). The energy ordering is taken from Bendale et al. (1992). Only two dipole allowed transitions originate from the $X\ ^2A_{1u}$ ground electronic state in D_{5d} symmetry, as shown by arrows representing 9632 Å (red) and 9577 Å (blue). There are more dipole allowed transitions (not indicated) from the $^2E_{1u}$ and the $^2E_{2u}$ states correlated with the $X\ ^2H_u$ manifold in I_h symmetry, some of which could overlap with the red and blue transitions observed.

(I_h) ground electronic state is split into three components: $^2A_{1u}$, $^2E_{1u}$, and $^2E_{2u}$ in D_{5d}. There are only two dipole allowed transitions from the $^2A_{1u}$ to the $^2E_{1g}$ states derived from ^2H_g and ^2G_g in I_h. However, further allowed transitions can occur from the low-lying $^2E_{1u}$ and $^2E_{2u}$ states correlated with ^2H_u.

In contrast to the spectrum of C_{60}^+–He, those of C_{60}^+–Ne and C_{60}^+–Ar show an additional resolved absorption band in the vicinity of 9632 Å (Figure 1, Holz et al. 2017). This may indicate a transition originating from a low-lying excited electronic state ($^2E_{1u}$ or $^2E_{2u}$). The implication for C_{60}^+ is that there could be more than one unresolved feature contributing to the 9632 Å absorption envelope. In this case the 9632/9577 EW ratio may increase with temperature due to the rise in relative population of the low-lying excited electronic state(s). A rigorous theoretical analysis of these features, to within spectroscopic accuracy, is a challenge for current computational methods.

2.2. The Astronomical Ratio

An exact match between the observed DIB ratios and those seen in the laboratory is hardly pivotal in the C_{60}^+ assignment because of the preceding discussion and contamination by other DIBs and stellar lines. Walker et al. (2016) detected three additional DIBs near the weaker members of the C_{60}^+ laboratory spectra at 9348, 9365, and 9428. The strengths of these companion DIBs appear uncorrelated with those assigned to C_{60}^+. There are several other weak DIBs throughout this spectral region and it is entirely possible that either or both of the 9632 and 9577 DIBs are blended with weaker, uncorrelated DIBs, introducing a natural scatter in their ratio. In fact, Galazutdinov et al. (2000) remarked that the 9577 DIB either has broad wings or is superposed on a broader DIB. Unfortunately, the Canada–France–Hawaii Telescope ESPaDOnS spectrograph (Donati 2003) has a narrow gap in spectral coverage coincident with the 9632 Å DIB, which prevented any measurements of it by Walker et al. (2016).

In a careful study in which the Mg II blend was removed using spectral standards, Jenniskens et al. (1997) reported a 9632/9577 EW ratio of 0.9 ± 0.05 based on observations of three reddened stars. Herbig (2000) measured a value close to unity for the heavily reddened O supergiant BD +40 4227A from the Keck I HIRES spectra using S Mon as the telluric standard. He pointed out that the 9632/9577 EW ratio is very sensitive to the spectral type of the telluric standard. His telluric standards were not rapid rotators.

Galazutdinov et al. (2000) made measurements of both DIBs with a variety of instruments and reported a value of unity for the 9632/9577 EW ratio with an estimated error of 20% after correction for the Mg II blend in the 9632 DIB, consistent with the 6 K laboratory result. There is some confusion in the way the results are presented since the points plotted in their Figure 6 do not correspond to the entries in their Tables 2 and 3. Here, in Figure 2, we re-plot the 9632 DIB values uncorrected (EW2) and corrected (EW2′) for the Mg II blend against the 9577 DIB. The values are taken from Tables 2 and 3 of Galazutdinov et al. (2000). One star, HD 183143, is plotted twice corresponding to observations at different sites. The two points for HD 183143 are connected by a short dotted line (an indication of the uncertainties). Least-squares and best-fitting straight lines (red) are shown together with the gradients (m) for each plot. Both the corrected and the uncorrected plots have gradients of 0.7 (±0.1) and correlation coefficients of 0.9. The uncorrected data have a 9632 zero-point offset of +56 mÅ, presumably corresponding to the average contribution of the Mg II blend.

Misawa et al. (2009) measured a ratio of 0.9 for two O-type stars in Orion. Being of such an early type there would have been little contamination by Mg II. Similarly, using the X-Shooter on the Very Large Telescope, Cox et al. (2014) measured a mean ratio of 1.1 (±0.1) for four reddened stars without any correction for the Mg II blend. They modeled the WV spectrum to correct for telluric line contamination.

All of these studies lead to a consistent agreement within errors and offsets—both laboratory and astronomical—with the laboratory prediction for the 9632/9577 EW ratio. This body of evidence was not considered by Galazutdinov et al. (2017) when they concluded from their analysis of the UVES data that the ratio, as they measured it, is much too variable to justify a single common absorber for the 9632 and 9577 DIBs. Although there are several lines of sight in common, Galazutdinov et al. (2017) did not compare any of their results with previous work. Here, we review their analysis.

We used the ESO Science Archive Facility's Spectral Data Products service to download processed spectra for three of the reddened stars used by Galazutdinov et al. (2017) with $T_{\rm eff} > 20{,}000$ (according to their Table 1). These stars are expected to have minimal Mg II blends. We also downloaded processed spectra for the two telluric standards, HD 130109 (A0V, $v\sin i = 351$) and Spica.

The UVES spectra are characterized by strong telluric contamination (an optical depth likely greater than 2 in the stronger lines). In Figure 3 we display UVES 9632 and 9577 DIB profiles for the three stars after normalization with the available telluric standard and rescaling to optimize reduction of the telluric lines. Our reduction procedure follows that

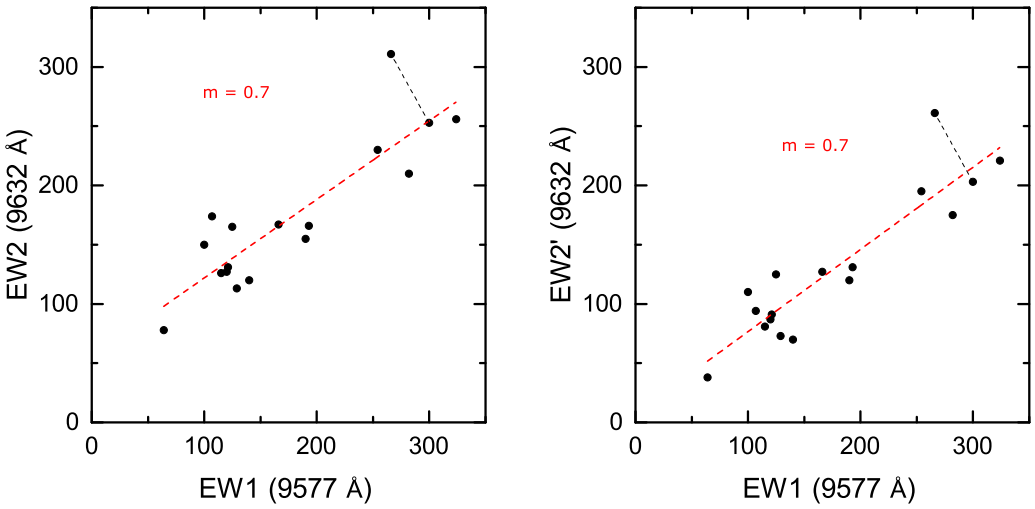

Figure 2. Plots of the 9632 and 9577 DIB equivalent widths (in mÅ) before (EW2) and after (EW2′) correction of the 9632 profile for the 9632.1 Å Mg II stellar blend. Data come from Tables 2 and 3 of Galazutdinov et al. (2000). There are two values for HD 183143 joined by a dashed line. The red line is the best-fitting straight line and m is the gradient.

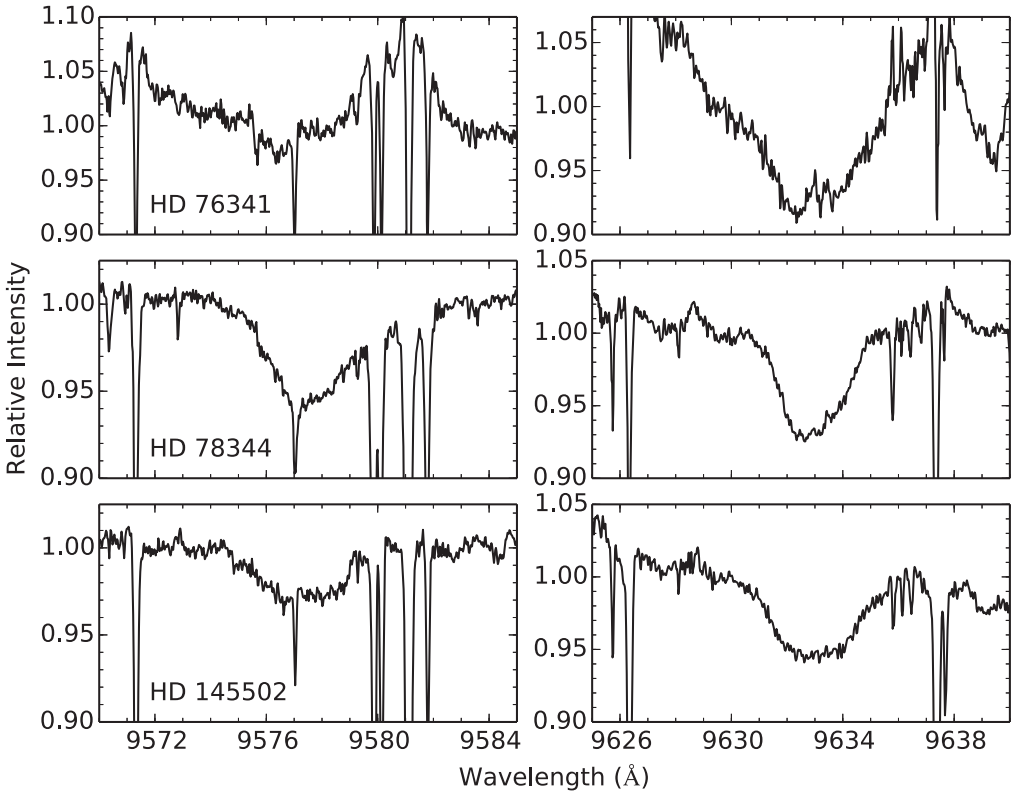

Figure 3. UVES spectra of the 9577 and 9632 EW DIBs for HD 76341, HD 78344, and HD 145502 after correction for telluric WV line contamination with the standard HD 130109. These illustrate the impact of incomplete WV correction in setting a continuum level. These three stars have $T_{\rm eff} > 20{,}000$ and consequently little Mg II stellar line contamination is expected in the 9632 DIB. These spectra are among those analyzed by Galazutdinov et al. (2017) . No interstellar wavelength offset has been applied.

outlined in Walker et al. (2015). It is clear that the impossibility of matching the strong WV lines between 9579.5 and 9582.0 Å in the program and standard stars has a major impact in setting the continuum level in that wing of the 9577 DIB. The 9632 DIB is also affected, but less seriously, in the long wavelength wing.

The UVES telluric standards reported in Galazutdinov et al. (2017) were not always taken at a similar air mass or even on the same night as the program stars. As a result, we could not properly correct, even with some scaling, for the telluric lines, many of which are saturated. The result is a serious distortion of the continuum as illustrated in Figure 3. We contend that it is not possible to properly restore the continuum (in agreement with Galazutdinov et al. 2000) and that the UVES 9632 and 9577 DIB profiles cannot be entirely trusted despite their high, formal S/N. It is worth comparing the spectrum of the 9632

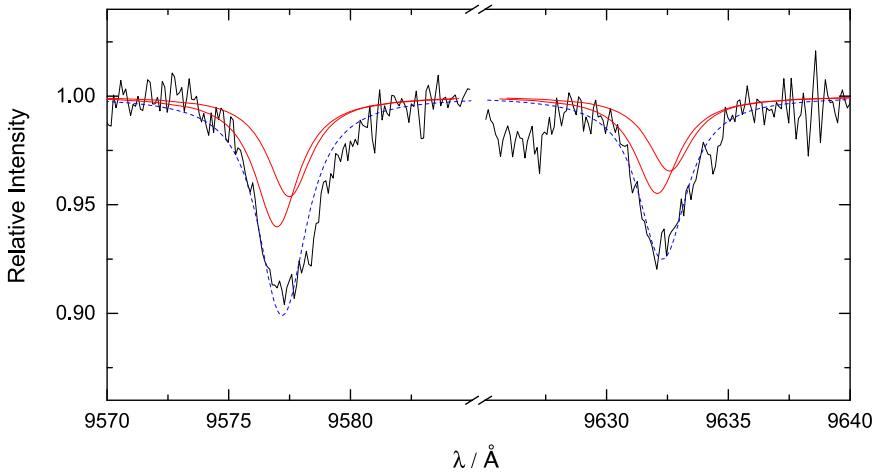

Figure 4. The 9577 and 9632 DIBs (black) in the spectrum of HD 183143 from Foing & Ehrenfreund (1997) corrected for telluric WV contamination and elimination of the 9632.1 Å Mg II stellar line blend using Rigel as the spectral standard. The wavelength scale is shifted by the average interstellar 7699.0 Å K line offset of -4.7 km s^{-1} (see Walker et al. 2016 for more details). A 2-cloud model is used where the red lines are Lorentzian fits to the astronomical data and the blue dashed line is the cumulative profile. The wavelengths and widths of the Lorentzians are constrained to the laboratory values. The best fits were obtained by allowing the fit parameters to vary by the quoted laboratory uncertainties. The 9632/9577 DIB intensity ratio is similar to that seen in the laboratory at 6 K.

and 9577 DIB in Figure 1 of Foing & Ehrenfreund (1997) taken with <0.25 mm of precipitable WV where despite a lower S/N the telluric lines have been completely eliminated, allowing confident assignment of a continuum. In Figure 4 we show fits to the 9632 and 9577 DIB with pairs of Lorentzian profiles corresponding to the two interstellar 7699.0 K line components reported by Walker et al. (2016). The 9632 DIB has been corrected for significant stellar Mg II line blending using spectra of Rigel for comparison (see Figure 1 in Walker et al. 2016) and corresponds to the EW2′ of Galazutdinov et al. (2000). In Figure 4 the 9632/9577 Å DIB ratio is 0.7, in agreement with the laboratory value, whereas Galazutdinov et al. (2017) obtained a value of 0.4 after making a larger correction for the Mg II blend from model atmosphere calculations.

There are three stars in common between Galazutdinov et al. (2000, 2017): HD 80077, HD 169454, and HD 183143. Overall the agreement in EW values reported in the two studies is not very good, particularly for the 9632 DIB (even before correction for the Mg II blend). This further undermines confidence in revising their earlier conclusions (Galazutdinov et al. 2000) based on the UVES spectra reported in Galazutdinov et al. (2017).

Concerning the comparison of DIB wavelengths with laboratory data, Galazutdinov et al. (2017, p. 3963) state that "...the disagreement of the central wavelengths with laboratory values needs to be addressed in order to defend the recently claimed identification of C_{60}^+." Although the authors provide no explanation of how their DIB wavelengths were obtained, we note that the 9577 DIB values in their Table 2 agree, within the quoted uncertainties, with the laboratory values (Campbell et al. 2016b) for 16 of the 19 target stars listed. The result for the 9632 DIB is similar.

3. Conclusion

The observational constraints on the astronomical measurement of the near-infrared DIBs attributed to C_{60}^+ have been discussed. Although data collected with ground-based telescopes under exceptionally dry conditions, or using the *Hubble Space Telescope,* can reduce or remove background telluric water contamination, corrections are also needed for stellar blends in the vicinity of the 9632 DIB. In addition, because of the large number of weak interstellar features found in this spectral region, either or both of the 9577 and 9632 DIBs may be overlapped by as-yet unidentified absorption bands. The latter would cause a spread in the EW ratio as measured along different lines of sight, thus making it difficult to establish a 9632/9577 EW variation. As discussed in this article, the results from the majority of astronomical studies, within the uncertainties caused by these observational constraints, are consistent with a constant 9632/9577 EW ratio. Nonetheless, it should be mentioned that due to the technique used the laboratory data were collected at 6 K, which is too low a temperature for nonpolar molecules in diffuse interstellar clouds (Indriolo et al. 2007). The effect of a higher internal temperature on the characteristics of the near-infrared C_{60}^+ electronic absorptions is considered. Laboratory spectroscopy at 30–100 K would be desirable, though currently the means to accomplish this is not evident. Because of the agreement of the wavelengths, FWHMs, and (approximate) relative intensities of five DIBs with the laboratory data, the identification of C_{60}^+ as a DIB carrier remains valid.

This work made use of the ESO Science Archive Facility services.

References

Bendale, R. D., Stanton, J. F., & Zerner, M. C. 1992, CPL, 194, 467
Campbell, E. K., Holz, M., Gerlich, D., & Maier, J. P. 2015, Natur, 523, 322
Campbell, E. K., Holz, M., Maier, J. P., et al. 2016a, ApJ, 822, 17
Campbell, E. K., Holz, M., & Maier, J. P. 2016b, ApJL, 826, L4
Cox, N. L. J., Cami, J., Kaper, L., et al. 2014, A&A, 569, A117
Donati, J.-F. 2003, in ASP Conf. Ser. 307, Solar Polarization, ed. J. Trujillo-Bueno & J. Sanchez Almeida (San Francisco, CA: ASP), 41
Edwards, S. A., & Leach, S. 1993, A&A, 272, 533
Foing, B. H., & Ehrenfreund, P. 1994, Natur, 369, 296
Foing, B. H., & Ehrenfreund, P. 1997, A&A, 317, L59
Fulara, J., Jakobi, M., & Maier, J. P. 1993, CPL, 211, 227
Galazutdinov, G. A., Krełowski, J., Musaev, F. A., Ehrenfreund, P., & Foing, B. H. 2000, MNRAS, 317, 750

Galazutdinov, G. A., Shimansky, V. V., Bondar, A., Valyavin, G., & Krełowski, J. 2017, MNRAS, 465, 3956
Herbig, G. H. 2000, ApJ, 542, 334
Holz, M., Campbell, E. K., Rice, C. A., & Maier, J. P. 2017, JMoSp, 332, 22
Indriolo, N., Geballe, T. R., Oka, T., & McCall, B. 2007, ApJ, 671, 1736
Jenniskens, P., Mulas, G., Porceddu, I., & Benvenuti, P. 1997, A&A, 327, 337
Langford, V. S., & Williamson, B. E. 1999, JCPA, 103, 6533
Kuhn, M., Renzler, M., Postler, J., et al. 2016, NatCo, 7, 13550
Maier, J. P., Lakin, N. M., Walker, G. A. H., & Bohlender, D. A. 2001, ApJ, 553, 267
Misawa, T., Gandhi, P., Hida, A., Tamagawa, T., & Yamaguchi, T. 2009, ApJ, 700, 1988
Sogoshi, N., Kato, Y., Wakabayashi, T., et al. 2000, JPCA, 104, 3733
Walker, G. A. H., Bohlender, D. A., Maier, J. P., & Campbell, E. K. 2015, ApJL, 812, L8
Walker, G. A. H., Campbell, E. K., Maier, J. P., Bohlender, D. A., & Malo, L. 2016, ApJ, 831, 130
Weeks, D. E., & Harter, W. G. 1991, CPL, 176, 209
Western, C. M. 2016, JQSRT, 186, 221
Yamada, K. M. T., Ross, S. C., & Ito, F. 2017, MolAs, 6, 9